Controlled Shift of Optical Bistability Hysteresis Curve and Storage of Optical Signals in a Four-Level Atomic System

Hong Chang, Haibin Wu, Changde Xie, and Hai Wang*

The State Key Laboratory of Quantum Optics and Quantum Optics Devices, Institute of Opto-Electronics, Shanxi University, Taiyuan, 030006, People's Republic of China

(Received 3 April 2004; published 16 November 2004)

The dependence of the shift of an optical bistability hysteresis curve on the nonlinear phase shift induced by a controlling light is observed in a four-level atomic system of ^{87}Rb inside an optical ring cavity. In the process the intensity of the coupling beam keeps constant and the atomic system is operated at near conditions of coherent population trapping due to atomic coherence. The refractive and absorptive $\chi^{(3)}$ nonlinearities enhanced by atomic coherence provide the physical mechanism of the phenomena. Based on the effects, all-optical flip-flop and storage of optical pulse signals with a low peak power of several tens of microwatts are implemented.

DOI: 10.1103/PhysRevLett.93.213901 PACS numbers: 42.65.Pc, 42.50.Gy, 42.65.Sf

In the past 20 years, optical bistability (OB) in two-level atomic systems has been extensively studied [1–5]. However, there are limitations for applications because of the lack of control due to only one laser beam being employed. It was discovered that electromagnetically induced transparency and coherent population trapping not only can modify the linear susceptibility of a medium but also can enhance the nonlinear optical processes in multilevel atomic systems [6–15]. The nonlinear optical processes related to the atomic coherence have shown their great potential in many interesting applications, such as slowing down the group velocity of light [8], trapping and manipulation of photon states [16–18], and cross-phase modulation for optical shutters [11]. It has been theoretically and experimentally demonstrated that, placing a multilevel electromagnetically induced transparency or coherent population trapping atomic system in an optical cavity to combine the nonlinear response of the atomic medium and optical feedback of the intracavity optical field, the Kerr-nonlinear interactions can be significantly enhanced [19,20]. A more intriguing effect, i.e., controlled threshold points of OB transition and the width of OB hysteresis curve by a coupling light in a three-level atomic medium, has been theoretically studied and experimentally observed [20,21]. However, there are no papers to clearly manifest the dependence of the shift of OB hysteresis curve on the nonlinear phase shift induced by a controlling light, and there are also no previous works to demonstrate that the OB can store optical data signals by means of the controllable shifts of OB curve resulting from the cross-phase nonlinearity in a four-level atomic system. In this Letter, we first display the dependence of the shift of OB hysteresis curve on nonlinear phase shift caused by a controlling light in four-level atoms inside an optical cavity. The observed effects are reasonably explained with the change of cavity resonant condition resulting from the enhanced cross-phase nonlinearity owing to atomic coherence via a simple physical model. We demonstrated that the OB hysteresis curve can shift toward different directions by two suitably tuned optical signals under the condition of keeping the intensity of the coupling light beam constant. For a given intensity of the probe beam, the OB system can be reliably changed from its lower stable state to the upper state under the triggering of an optical signal pulse (named up-controlling signal). More interestingly, the inverted OB upper state does not drop to its initial lower stable state after the triggering signal pulse ends, but moves to the upper branch of the initial OB curve and stably stays there until another optical signal, tuned to another atomic transition (named down-controlling signal) comes by. These results show the possibility of information storage in the current four-level atomic OB system. The new mechanism of information storage might have important applications in the all-optical information processing.

We consider a four-level ^{87}Rb atomic system as shown in the inset of Fig. 1. The hyperfine levels $F = 1$ and $F = 2$ of the ground state of $5S_{1/2}$ serve as the two lower states $|1\rangle$ and $|2\rangle$, respectively. The hyperfine levels $F' = 2$ of $5P_{1/2}$ state and $F' = 2$ of $5P_{3/2}$ state serve as the two upper states $|3\rangle$ and $|4\rangle$, respectively. The coupling light and the down-controlling signal with same frequency ω_c (but orthogonally polarized) both couple to the transition from $|2\rangle$ to $|3\rangle$. The up-controlling optical signal of frequency ω_u couples to the transition from $|1\rangle$ to $|4\rangle$. The probe laser of frequency ω_p interacts with states $|1\rangle$ and $|3\rangle$. LD1, LD2, and LD3 are three extended-cavity diode lasers, and their frequencies are stabilized with three saturation absorption spectroscopy setups. The optical ring cavity consists of a flat mirror M1 with 99.5% reflectivity and two concave mirrors, M2 and M3, of $R = 10$ cm with reflectivities of 95% and 99.5%, respectively. The mirror M3 is mounted on a piezoelectric transducer for scanning and locking the length of the cavity. The Rb vapor cell (5 cm in length and heated to 62 °C) with

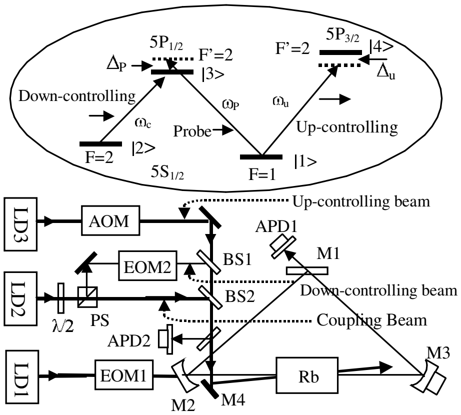

FIG. 1. Experimental setup and diagram of atomic levels. PS: polarizing beam splitter; $\lambda/2$: half-wave plate; APD1, APD2: avalanche photodiode detectors.

wrapped μ-metal sheet is placed inside the cavity on the center position between M2 and M3. The finesse of the empty cavity is about 100 with a free spectral range of 870 MHz (cavity length is 34.5 cm) and is degraded to about 32 (with Rb atoms far off resonance) when the Rb vapor cell with the reflection losses (12%) from its two windows is inserted. The probe laser from LD1 passes through an electro-optical modulator (EOM1) and then enters the cavity through M2 to circulate inside the optical ring cavity. The LD2 laser is split by a polarizing beam splitter to two parts; one of them serves as the coupling light and the other one passes through EOM2 as a down-controlling optical signal. The laser from LD3 passes through an acoustic-optical modulator and serves as the up-controlling optical signal. The controlling and the coupling beams are combined at the beam splitters BS1 and BS2, which are then introduced into the Rb vapor cell by a high reflection mirror M4. The orientation of these beams is misaligned by a small angle (about 1°) to avoid their circulation inside the optical cavity. The polarizations of both up-controlling and down-controlling beams are parallel to that of the probe light, and the polarization of the coupling light is perpendicular to other beams to avoid its interfering with the down-controlling beam of the same frequency. The ring cavity length is locked to a Fabry-Perot reference cavity with an extra diode laser (not shown Fig. 1), the frequency of which is far from the absorption lines of the atoms. The radii of the probe, coupling, and down-controlling and up-controlling beams are estimated to be 130 μm, 280 μm, 380 μm, and 150 μm at the center of the Rb cell, respectively. The probe light (795 nm) is locked around the atomic transition frequency ω_{31} from $|1\rangle$ to $|3\rangle$ with a detuning of $\Delta_p = \omega_p - \omega_{31} = 70$ MHz. The coupling and down-controlling beams (795 nm) are locked onto $|2\rangle$ to $|3\rangle$ transition frequency ω_{32} with zero detuning ($\Delta_c = \omega_c - \omega_{32} = 0$). The up-controlling beam (780 nm) is locked onto $|1\rangle$ to $|4\rangle$ transition frequency ω_{14} with a detuning of $\Delta_u = \omega_u - \omega_{41} = -16$ MHz. In the atomic cell, the introduced coupling and two controlling beams propagate in the same direction as the probe light to eliminate the first-order Doppler effect [7].

At first, we studied the dependence of the shift of OB hysteresis curve on the nonlinear phase shift caused by a controlling light and found that the OB hysteresis curve shifts toward left or right correspond to the positive or negative nonlinear phase shift, respectively. We measured the shift of the cavity resonant peak induced by the controlling light using the method described in Ref. [15]. The transmission curve a in Fig. 2(a) was obtained only with the probe (1.1 mW) and coupling (130 μW) beams on without the controlling light signals. When turning the up-controlling light of 70 μW on, the transmission curve shifted to c (toward the left). Instead of the up-controlling light, when the down-controlling beam of 270 μW was turned on, the curve shifted to b (toward the right). Utilizing the measured shift amounts of the resonant peak from a to b or c, we obtained the nonlinear phase shifts caused by the up-controlling or down-controlling light to be $\delta\theta_u \approx 2\pi/40$ and $\delta\theta_d \approx -2\pi/30$ [15], respectively, which correspond to the nonlinear

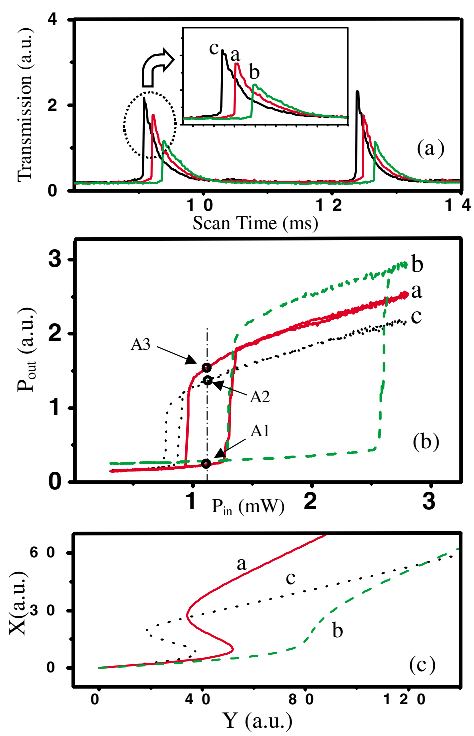

FIG. 2 (color online). (a) Cavity transmission profile. (b) Experimental OB hystersis curves. Curve a: without up- and down-controlling light; curve b: with down-controlling light; curve c: with up-controlling light. (c) Calculated OB hystersis curves. Parameters are $C = 60$, $\delta_p = 11$, for curve a: $A = 0$, $\Phi = 0$; curve b: $A = 0.6$, $\Phi = -2.2$; curve c: $A = -0.3$, $\Phi = 1.6$.

refractive parameters $\Phi_u \approx 1.6$ rad and $\Phi_d \approx -2.2$ rad [see Eq. (4)]. Thus, the cross-phase Kerr-nonlinear refractive indexes are $n_{2,u} \approx 3.9 \times 10^{-6}$ cm^2/W and $n_{2,d} \approx -8.9 \times 10^{-6}$ cm^2/W [15], respectively. The absorption losses in a single pass are estimated to be about 12%, 18%, and 9%, respectively, for the three cases of cavity transmission *a*, *b*, and *c*. The corresponding changes of absorptive parameter of the probe field induced by the up-controlling and the down-controlling light are $A_u \approx -0.3$ and $A_d \approx +0.6$ [see Eq. (3)], respectively.

We then locked the length of cavity at a cavity phase detuning of $\theta = 0.1$ rad to the resonant peak of the probe beam and scanned the input power of the probe beam with EOM1 to observe the OB. In the meantime, the power of the coupling light was kept at 130 μW to achieve the enhancement of Kerr nonlinearity in the medium owing to atomic coherence [20]. The three OB hysteresis curves in Fig. 2(b), i.e., the solid line *a*, the dashed line *b*, and the dotted line *c*, are obtained at different conditions, corresponding to the conditions producing cavity transmissions *a*, *b*, and *c* in Fig. 2(a), respectively. The results show that the threshold points of OB shift toward higher intensity of probe light (right) and the region of OB becomes wider under the action of the down-controlling light with a power of 270 μW. With the down-controlling light off and the up-controlling light (70 μW) on, the OB curve shifts toward left (the threshold powers decrease) and the region of OB is narrowed.

In the following we briefly analyze the physical mechanism of the above experimental results with the nonlinear susceptibility and the state equation of OB. For the coupling and controlling lights at low intensities, the total susceptibility in the four-level atomic system can be approximately expressed by

$$\chi \approx \frac{\alpha_0}{k_p} \frac{i - \delta_p}{1 + \delta_p^2 + I_p/I_{sat}} + \chi^{(3)}_{u(d)} |E_{u(d)}|^2, \qquad (1)$$

where α_0 and k_p stand for the absorption coefficient and the wave vector of the probe light, respectively. I_p is the intensity of the intracavity probe light and I_{sat} is the saturation intensity of the atomic vapor. $\delta_p = (\Delta_p + \omega_p v/c)/\gamma_\perp$ is the normalized atomic detuning of the probe light (v is the flight velocity of atom, $\gamma_\perp$ is the atomic resonance half-width, and c is the velocity of light). $\chi^{(3)}_{u(d)}$ is the third-order nonlinear susceptibility of the medium at the frequency of the probe light, which responds to the up- (down-)controlling light. $E_{u(d)}$ is the average amplitude of the up- (down-)controlling light field. The third-order nonlinear polarization $\chi^{(3)}_{u(d)} |E_{u(d)}|^2$ enhanced by atomic coherence in multilevel atomic system [8,11–15] directly results in the large phase shift of intracavity probe field based on the cross-phase modulation, which is why the OB curve can shift under the triggering of the controlling lights with low intensities. Substituting Eq. (1) into Airy's equation [22], we obtain the input-output relation of the optical cavity with the four-level atomic system as

$$Y = X\{[1 + A_{u(d)} + 2C/(1 + \delta_p^2 + X)]^2 + [\Theta + \Phi_{u(d)} - 2C\delta_p/(1 + \delta_p^2 + X)]^2\}, \qquad (2)$$

where $Y = I_{in}T_1/[(1 - \overline{R})^2 I_{sat}]$ and $X = I_{out}/(T_2 I_{sat})$ are the normalized input and output intensities, respectively. $\overline{R} = \sqrt{(1 - T_1)(1 - T_2)T_c}$ plays the role of an average reflectance in the expression. T_1, T_2, and T_c stand for the transmissivities of M1, M2, and the two windows of Rb cell, respectively. The cavity detuning Θ is $\Theta = F\theta$, here $F = \overline{R}/(1 - \overline{R})$, and $\theta = k_p L - 2m\pi$ is the phase detuning of the cavity (L is the length of the cavity and m, integers). $C = \alpha_0 l F/4$ is the atomic cooperation parameter (l is the length of the Rb vapor cell). The absorptive and refractive parameters $A_{u(d)}$ and $\Phi_{u(d)}$ are proportional to the imaginary and the real parts of the third-order nonlinear susceptibility at the frequency ω_p given by:

$$A_{u(d)} == F \mathrm{Im}[\chi^{(3)}_{u(d)}(\omega_p)|E_{u(d)}|^2] k_p l/2 = F\delta\alpha_{u(d)}, \qquad (3)$$

$$\Phi_{u(d)} = F \mathrm{Re}[\chi^{(3)}_{u(d)}(\omega_p)|E_{u(d)}|^2] k_p l/2 = F\delta\theta_{u(d)}, \qquad (4)$$

where $\delta\alpha_{u(d)}$ and $\delta\theta_{u(d)}$ describe the modifications of the absorption loss and the phase shift of the probe light resulting from the controlling light in a single pass, which are measured in the experiment. The simulation calculations from Eq. (2) with the parameters measured in the experiment are shown in Fig. 2(c). The move of the threshold points and the change of OB hysteresis curve are due to the changes of absorptive and refractive parameters induced by the controlling lights. The differences between the theoretical and experimental figures are due to the fact that the detailed Doppler broadening effect was not considered in the calculation which existed, however, in the real experiment.

Blocking two controlling lights and keeping the power of the probe light at 1.1 mW, the output from the cavity stays at the state *A*1 with a power close to zero (lower branch of curve *b* in Fig. 2(b)]. Then, as the up-controlling beam is turned on, the system jumps to state *A*2 (upper branch of curve *c*) with an output power of ~1.5 μW because the up-switching threshold power of OB curve *c* is reduced to below the holding power of the probe light (1.1 mW). As the up-controlling beam is turning off, the intracavity field continually evolves into state *A*3 (upper branch of curve *a*) without any interruption. In such case, the system will not jump back down to the lower state *A*1, since no external signal is added to activate switching among different branches of a bistable curve [23]. After the up-controlling beam turns off completely, the state *A*3 can be stably maintained if no external disturbance is applied. When the down-

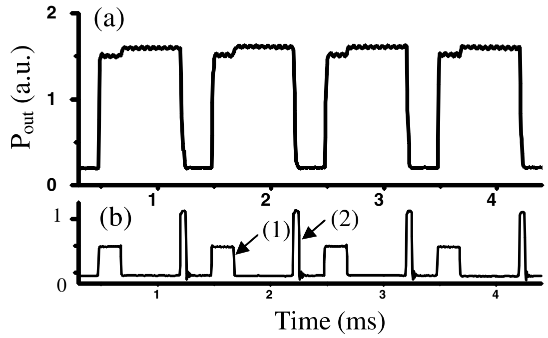

FIG. 3. Optical switching and storage. (a) Transmission power of the probe light from the optical cavity; (b) controlling pulse sequence: (1) up-controlling signal and (2) down-controlling signal.

controlling light is turned on in a later time, the system jumps back to $A1$ from $A3$ because the down-switching threshold power of OB curve b is raised beyond 1.1 mW.

Utilizing the above effects, we demonstrated the switching and storage ability of the OB system in this four-level atomic system under the alternate triggering of the up- and down-controlling optical pulses. Figure 3(a) records the change of the transmission power of the probe light from the optical cavity under the triggering of the controlling lights, and Fig. 3(b) shows the corresponding controlling pulse sequence [(1) corresponds to up-controlling signal and (2) corresponds to down-controlling signal]. The peak power and the duration of each of the up-controlling (down-controlling) pulse signals were 70 μW (270 μW) and 200 μs (50 μs), respectively. The small step on the high output power in Fig. 3(a) corresponds to the move of the output power from point $A2$ to $A3$ after the up-controlling signal pulse is over. It is obvious that the states of the OB system can be quickly switched with two controlling pulses. [The fastest switching speed (3 μs) in our experiment was limited by the response speeds of the available acoustic-optical modulator and EOM in our present system.] The pulse information can be reliably maintained in the OB system after the triggering of the optical up-controlling pulse ends.

We would like to point out that the present switching process in the OB system is quite different from the demonstrated all-optical switching in Ref. [24], in which the cavity transmission power can be just switched ''on ''and ''off '' with two different values of the frequency detuning (or intensity) of coupling beam, so it can only work as an all-optical switch without any memory ability.

In conclusion, we observed the controllable shift of the threshold points and the change of the hysteresis curve of OB induced by two suitably tuned lights in a four-level ^{87}Rb atomic system inside an optical ring cavity under a constant input probe power for the first time. The switching and information storage performances were observed under the triggering of the optical signal pulses with the peak power of only several tens of microwatts. The low power operation of the system and the increase of the controllable factors make the presented OB system more valuable for applications in all-optical switches, information storage, and logic circuits of all-optical information processing.

This research was supported by NSFC Grant No. 60325414, NSFC Grants No. 60238010 and No. 19974021, and Major State Basic Research Project of China Grant No. 2001 CB309304.

*Email address: wanghai@sxu.edu.cn.

[1] H. M. Gibbs *et al.*, Phys. Rev. Lett. **36**, 1135 (1976).
[2] A. T. Rosenberger *et al.*, Phys. Rev. A **43**, 6284 (1991).
[3] G. Rempe *et al.*, Phys. Rev. Lett. **67**, 1727 (1991).
[4] A. Lambrecht *et al.*, Opt. Commun. **115**, 199 (1995).
[5] T. Ackemann *et al.*, Phys. Rev. A **56**, 2321 (1997).
[6] S. E. Harris, Phys. Today **50**, 36 (1997).
[7] Y. Li and M. Xiao, Phys. Rev. A **51**, R2703 (1995).
[8] L. V. Hau *et al.*, Nature (London) **397**, 594 (1999).
[9] H. Wang *et al.*, Phys. Rev. Lett. **87**, 73601 (2001).
[10] H. Wang *et al.*, Opt. Lett. **27**, 258 (2002).
[11] H. Schmidt and A. Imamoglu, Opt. Lett. **21**, 1936 (1996).
[12] S. E. Harris and Y. Yamamoto, Phys. Rev. Lett. **81**, 3611(1998).
[13] H. Kang and Y. Zhu, Phys. Rev. Lett., **91** 093601 (2003).
[14] D. A. Braje *et al.*, Phys. Rev. A **68**, R041801 (2003).
[15] H. Chang *et al.*, Europhys. Lett. **65**, 485 (2004).
[16] C. Liu *et al.*, Nature (London) **409**, 490 (2001); D. F. Phillips *et al.*, Phys. Rev. Lett. **86**, 783 (2001).
[17] A. S. Zibrov *et al.*, Phys. Rev. Lett. **88**, 103601 (2002).
[18] C. H. van de Wal *et al.*, Science **301**, 196 (2003); A. Kuzmich *et al.*, Nature (London) **423**, 731 (2003).
[19] A. Imamoglu *et al.*, Phys. Rev. Lett. **79**, 1467 (1997).
[20] A. Joshi *et al.*, Phys. Rev. A **67**, R041801 (2003).
[21] W. Harshawardhan and G. S. Agarwal, Phys. Rev. A **53**, 1812 (1996); A. Joshi *et al.*, Phys. Rev. A **68**, 015806 (2003).
[22] W. Boyd, *Nonlinear Optics* (Academic, New York, 1992).
[23] A. Brown, A. Joshi, and M. Xiao, Appl. Phys. Lett. **83**, 1301 (2003).
[24] H. Wang *et al.*, Phys. Rev. A **65**, 051802 (2002); H. Wang *et al.*, Opt. Lett. **27**, 1354 (2002).